

# PHYSICAL REVIEW B

## SOLID STATE

THIRD SERIES, VOL. 7, No. 10

15 MAY 1973

### Optical Properties of Niobium from 0.1 to 36.4 eV

J. H. Weaver, D. W. Lynch, and C. G. Olson

*Ames Laboratory, U. S. Atomic Energy Commission and Department of Physics,  
Iowa State University, Ames, Iowa 50010*

(Received 22 September 1972)

The absorptivity or reflectivity of single crystals of Nb has been measured from 0.1 to 36.4 eV. The data were Kramers-Kronig analyzed and the optical constants obtained. The absence of low-energy interband transitions has been noted, while interband effects have been observed beginning at about 1.4 eV and extending to about 19 eV. Comparisons with existing experimental data are made. Identification of some interband effects has been tentatively made from the band structure calculated by Mattheiss. The loss function has been obtained and strong resonances have been noted at 9.9 and 20.8 eV. From our spectra of the complex dielectric constant, we can identify both of these as being plasmon excitations. The onset of core transitions at about 28 eV has been observed.

#### INTRODUCTION

Optical measurements are of considerable value in the study of the electronic properties of materials. A variety of different experimental approaches is taken, but the goal is to determine the complex index of refraction  $\tilde{N}$ , or the complex dielectric function  $\tilde{\epsilon}$ , where  $\tilde{\epsilon} = \epsilon_1 + i\epsilon_2$ . A knowledge of the real and imaginary parts of  $\tilde{\epsilon}$  is of particular importance to those interested in band structures. Since  $\epsilon_2$  is a measure of the interband transition strength, information concerning the density of states, as well as the location of the bands relative to one another and to the Fermi level, can be obtained. Given optical data, it is possible to adjust calculational parameters to obtain agreement; if the bands are known, the experimental data allow a check as to their accuracy.

A considerable amount of experimental data on the simple metals and nontransition metals exists in the literature. Energy-band-calculation schemes have been developed and the electronic properties are known rather well. For the transition metals, however, this is not the case. Band calculations have historically been hampered by the very nature of the transition metals, i. e., the existence of nonlocalized  $d$  electrons. In recent years there has been much activity in devising en-

ergy-band-calculation schemes and constructing appropriate potentials to be used for the transition metals.<sup>1-7</sup> It appears timely, then, for a comprehensive experimental study of a series of the transition metals. Such a study has been undertaken; the present paper represents the first of the series.

The existing optical data on the transition metals in general, and on Nb in particular, are limited in a number of respects. Most studies have been restricted to a relatively small energy range, and a composite of several such works is needed for a complete spectrum. This is often complicated by disagreement from group to group. In addition, it has been only recently that one has been able to perform accurate measurements at high energies, except perhaps at a very few points. Further, there are many studies carried out by ellipsometry, but it is only within the last few years that the technique has been developed to the point where the data are reliable when the sample is below room temperature. The question of sample preparation further complicates the interpretation of published data. It is now established that a work-damaged layer must be removed chemically from the sample surface following mechanical polishing, and that care must be taken to reduce the formation of oxide layers. In particular, recent papers have argued that as much as 180  $\mu\text{m}$  of surface must be

removed from a sample,<sup>8,9</sup> the amount varying from element to element.

The most recent optical work with Nb was that of Golovashkin, Leksina, Motulevich, and Shubin (GLMS).<sup>10</sup> They employed an ellipsometric technique in the 0.4–10- $\mu\text{m}$  range, and made measurements at 293, 78, and 4.2 °K. Considerable attention was given to sample preparation, and it was reported that surface damage extended a depth of 50  $\mu\text{m}$  into the surface. An electropolish was used to remove this worked layer. The earlier work by Vilesov, Azgrubskii, and Kirillova<sup>11</sup> (VAK)<sup>11</sup> also recognized the need for chemical polishing. They reported a reflectivity spectrum that extended from 3.1 to 14.3 eV. A room-temperature photoemission technique was used. Other early work<sup>12</sup> was carried out with samples that were merely mechanically polished, and are less representative of an unstrained Nb crystal lattice.

A variety of experimental information has recently been obtained about the Fermi surface of Nb. Galvanometric,<sup>13</sup> magnetothermal oscillation,<sup>14</sup> and de Haas–van Alphen<sup>14,15</sup> measurements have been performed. From the theoretical point of view, the electronic structure has been considered by Mattheiss<sup>7</sup> and earlier by Deegan and Twose.<sup>6</sup>

In the present paper optical data which extended from 0.1 to 36.4 eV are presented, and a comparison is made with the existing data mentioned above. We then analyze our data and present the optical constants. Finally, the data are discussed in terms of the band structure of Mattheiss.<sup>7</sup>

### I. EXPERIMENTAL METHOD

The data presented here were obtained with three sets of apparatus. A calorimetric technique was used in the infrared, through the visible and into the ultraviolet (0.1–4.5 eV), and the absorptivity was measured at 4.2 °K and 15° angle of incidence. In the vacuum ultraviolet, synchrotron radiation from the electron storage ring (operated by the Physical Sciences Laboratory of the University of Wisconsin) was used; room-temperature reflectivity data were obtained from 5 to 36.4 eV at 10°, 45°, and 60° using *s* and *p* polarizations. To provide a region of overlap, a Cary 14R spectrophotometer<sup>16</sup> was used to determine the reflectivity from 0.7 to 6 eV. The relative accuracies are estimated to be  $A = \pm 1\%$  at 1 eV for the calorimeter,  $R = \pm 2\%$  for the Cary,<sup>17</sup> and  $R = \pm 5\text{--}10\%$  for the storage ring. Details of the experimental technique and the equipment used are discussed elsewhere.<sup>18</sup>

Samples of niobium were prepared from material obtained within the Ames Laboratory of the AEC. It was subsequently electron-beam melted, and a chemical analysis showed the following impurities

(ppm): C, 8; O, 9.6; N, 11; Ta, <150; and Ti, <100. (The latter two values represent the limit of sensitivity of analysis.) No Al, Ca, Cu, Fe, Mg, Ni, or Si were detected. Single crystals were spark cut from the beam-melted ingot. The samples were mechanically polished with abrasives, the final grade being a paste of 0.05- $\mu\text{m}$ -diameter alumina. They were then sealed in an evacuated Ta capsule and annealed for 18 h at 1650 °C. Finally, they were very lightly polished with 0.05- $\mu\text{m}$  alumina, and either chemically polished or electropolished. Since GLMS reported that at least 50  $\mu\text{m}$  of surface should be removed, we were very careful to remove at least that much. Initially, a chemical polish was used (HF : HNO<sub>3</sub> : : 1 : 1); later an electropolish was used (2% H<sub>2</sub>SO<sub>4</sub> in methanol at –70 °C). The results were practically identical. While GLMS noted that formation of an oxide layer proceeds very slowly, we routinely mounted the sample in a vacuum chamber and evacuated it as quickly after electropolishing as possible (about 15 min before 10<sup>–4</sup> Torr; within 30 min cooling was initiated for calorimetry).

### II. RESULTS

In Fig. 1 we display our measured absorptivity in the range 0.1–6 eV. Also shown are the data of Golovashkin, Leksina, Motulevich, and Shubin,<sup>10</sup> as calculated from their published *n* and *k* values. It should be noted that the lines associated with these latter data were drawn by us and are not necessarily exactly as GLMS might have drawn them. Also shown in Fig. 1 are the data of Vilesov, Azgrubskii, and Kirillova (VAK).<sup>11</sup>

In Fig. 1 we see that the agreement of our *uv* data with those of VAK is reasonably good. Structures in *A* at about 3.75 and 4.8 eV are evident in both sets of data. The shoulder we observe at about 1.8 eV is also apparent in the data of GLMS; our *A* data appear to be roughly 5% higher than theirs. The results of GLMS and VAK clearly disagree at 3.1 eV, both in magnitude and slope, but this is the end of the experimental range of both groups. An examination of the data points of the former show the hint of a rise in *A* around 2.8 eV. If the data above 2.8 eV were disregarded, an extrapolated curve might easily be drawn to the data of VAK that would run nearly parallel to ours.

An expanded low-energy region allows a better comparison of our data with those of GLMS. In the insert of Fig. 1 we show the three sets of GLMS data as well as our own. A comparison of our curve with the 293 °K data is favorable. They observe no structure at 293 °K. However, the peaks at about 0.38 and 0.56 eV, which they observe at 78 and 4.2 °K, have not been detected at all by us; if such structures existed, they would have been

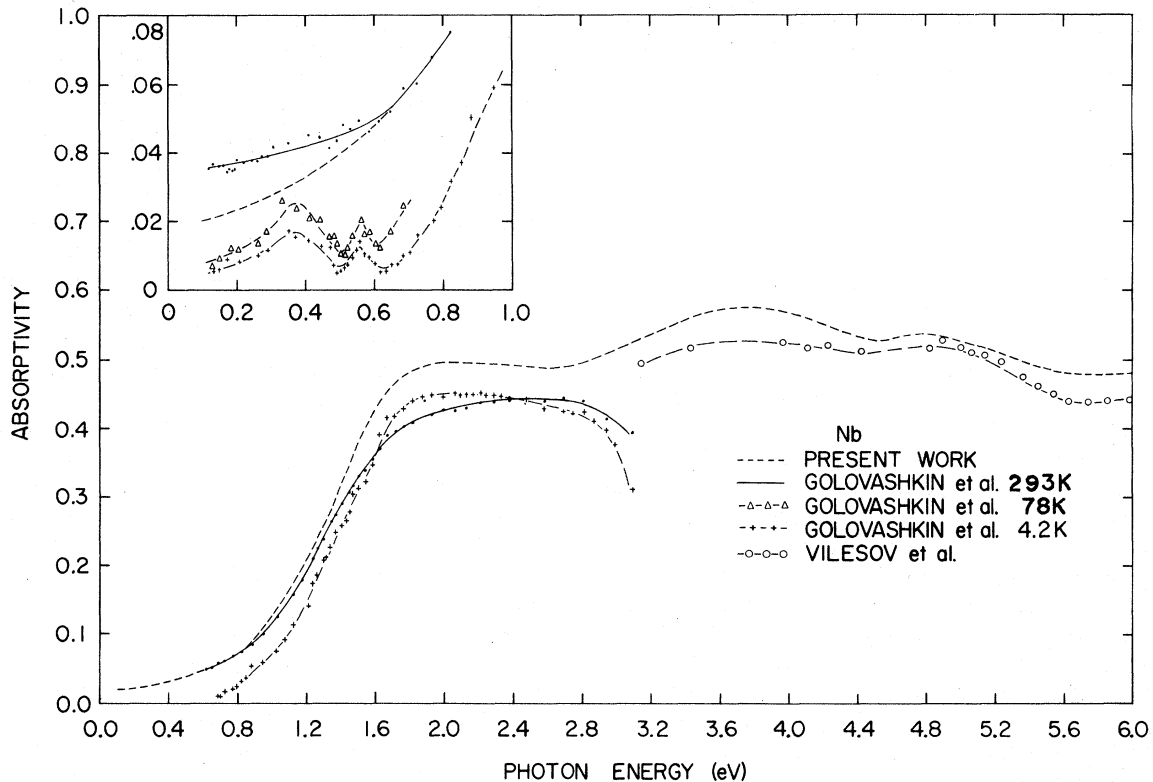


FIG. 1. Absorptivity of niobium at  $15^\circ$  angle of incidence. The data to 4.5 eV were taken at 4.2 K. The insert shows the low-energy region.

clearly evident. In earlier papers the existence of structure in Zn,<sup>19</sup> Cd,<sup>20</sup> and Al<sup>21</sup> has been reported at 0.15, 0.29, and 0.40 eV, respectively. In Ni,<sup>22</sup> slight changes in slopes have been noted. We thus have considerable confidence in the reliability and sensitivity of our apparatus. It is clear that virtually no structure in Nb below the onset (at about 1 eV) has been observed. We suspect that the structure reported may have arisen from condensates on the samples at low temperature; ellipsometry is very sensitive to surface contamination.

It can be said that the disagreement results from different sample preparation. Heeding the caution of GLMS regarding removal of surface damage, we have been careful to remove amounts in excess of 50  $\mu\text{m}$ . In an extreme case, a crystal was chemically reduced from 2.7 to 0.5 mm in thickness. The results obtained were the same as those presented in Fig. 1, to within experimental error. Since it has been shown that an oxide layer forms very slowly on Nb,<sup>10</sup> any differences from that quarter can be disregarded, though ellipsometry is certainly more prone to error from such films than is calorimetry. This is also true for a condensate on the surface. In calorimetric measurements performed at  $15^\circ$  angle of incidence, the ef-

fect of any condensed transparent gas is negligible. Nonetheless, we were careful to delay cooling to 77° K until the vacuum was  $10^{-5}$  Torr or better. Our sample was thermally connected to the refrigerant only by a single 20-cm-long No. 32 Cu wire and was the last part of the cryostat to cool. Since ion pumps were used, there was no danger of oil vapors contaminating the surface. At any rate, these problems would be more likely to introduce structure than to obscure it.

The complete reflectivity spectrum of Nb from 0.1 to 36.4 eV is shown in Fig. 2. The insert shows an expanded section of the spectrum and includes an extrapolation which was introduced above 36.4 eV to bring the reflectivity back to zero. A considerable amount of structure is evident from the figure. The reflectivity is seen to drop smoothly to 50.3% at 2.0 eV, rise through a shoulder at 2.6 eV, pass through a minimum at 3.8 eV, and form a broad hump at 5.8 eV which has shoulders at 4.5 and 7.7 eV. It then drops smoothly to a minimum at 10.3 eV, which is followed by a hump at about 11.7 eV. Also seen is a slight shoulder on the high-energy side of the broad hump at 16 eV, occurring at about 20.7 eV. The reflectivity passes through a minimum of 1.5% at 27.8 eV, displays a kink at 30.6 eV, and continues

to rise beyond the limit of our data. The rise in reflectivity above 28 eV and the small structure at 30 eV are genuine. Scattered and second-order light represent less than 1% of the beam incident on the sample.<sup>18</sup> The shape of the reflectivity curve above 28 eV is the same when measured with or without a thin-film Al transmission filter.

The standard form of the Kramers-Kronig (KK) integral calls for reflectivity data over an infinite range of frequencies. It is customary to truncate the integral at both high and low energies. Experimental data are taken in the range where they are known and extrapolations are made elsewhere. For the present work, we were able to provide reflectivity data continuously from 0.1 to 36.4 eV. To KK analyze, then, we extrapolated in the infrared by assuming a Drude-like behavior, and in the ultraviolet by forming the maximum in  $R$  at 38.5 eV and forcing  $R$  to drop off smoothly to zero at high energy. The reason for this choice will be discussed later. The phase angle was then evaluated and the optical constants were calculated, assuming  $10^\circ$  angle of incidence and perfect polarization. (The synchrotron radiation was  $\sim 88\%$  polarized.) The resultant spectrum of the complex dielectric constant  $\tilde{\epsilon}$  was used to compute the  $s$  and  $p$  reflectivity at  $45^\circ$  and  $60^\circ$ , assuming incomplete polarization. These were compared with our measured values. Agreement was surprisingly good below 10 eV in all cases, and below 16 eV in all but the  $60^\circ$ - $p$  case. At 21 eV disagreement ap-

peared. (The calculated reflectivities were too low.) Thus the magnitudes of  $\epsilon_1$  and  $\epsilon_2$  become less reliable above 21 eV, but their shapes may still be correct. The effect of the extrapolation on the dielectric constants is discussed later.

In Fig. 3 we display the real and imaginary parts of the complex dielectric function  $\tilde{\epsilon}$ . The vertical scale for  $\epsilon_2$  is enlarged by a factor of 10 below 6 eV in order to show the low-energy structure. It is seen that  $\epsilon_2$  drops smoothly from a large, positive, free-electron value in the infrared and passes through a minimum at 1.4 eV, thus marking the onset of dominance by interband rather than intraband effects. Subsequently, maxima are observed at 2.4, 4.3, 5.1, 11.4, and 13.8 eV with shoulders visible at 7.6, 20, and 30.4 eV. A rise is seen around 37 eV but the shape is affected by our choice of high-energy extrapolation. While the structure can be identified as due to core transitions, the peak position and magnitude are only qualitatively correct.

Also shown in Fig. 3 is the real part of  $\tilde{\epsilon}$ . It is seen to rise steeply, cross the axis at 1.95 eV, and peak at 2.2 eV. Maxima are then observed at 4.0, 10.6, and 13 eV with shoulders at about 4.8 and 7.2 eV. Minima occur at 3.8, 5.8, and 16.4 eV. Five more zero crossings occur. A kink in  $\epsilon_1$  is observed at 20.8 eV and another appears at about 30.5 eV.

The electron energy-loss function, defined as  $\epsilon_2/(\epsilon_1^2 + \epsilon_2^2)$ , is shown in Fig. 4. The large spike

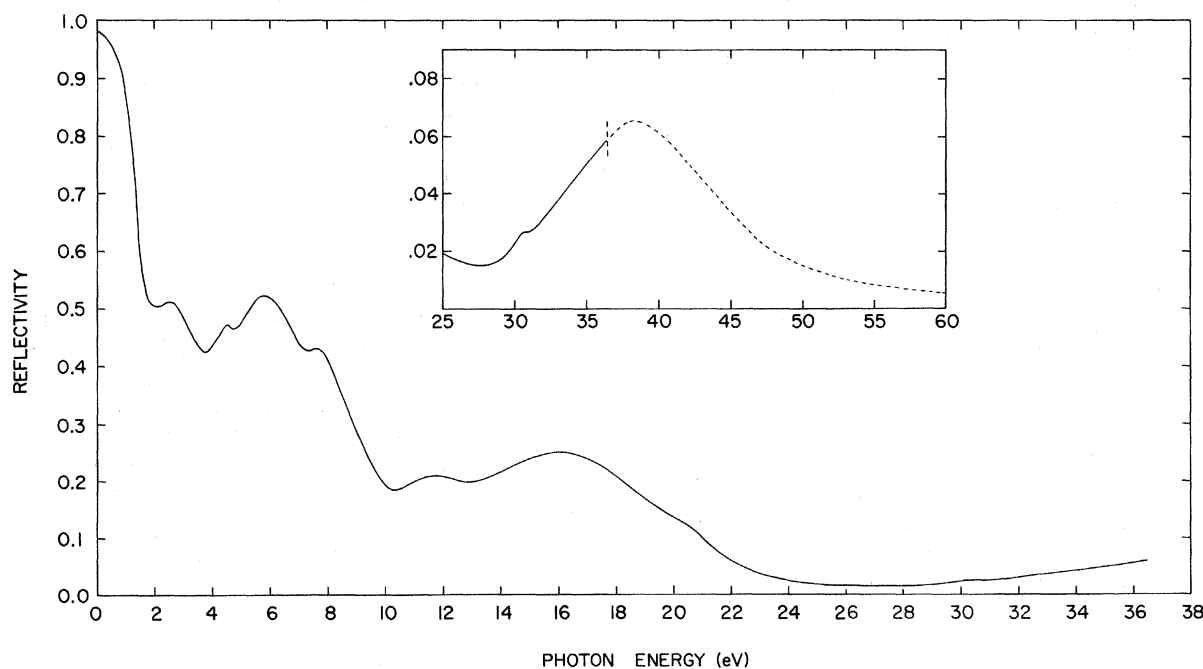


FIG. 2. Reflectivity spectrum of niobium. The insert presents an expanded high-energy range and includes the extrapolation used beyond 36.4 eV.

at about 20.9 eV dominates, through numerous other features are also identifiable. The origin of these structures will be discussed subsequently. The surface loss function  $\epsilon_1/[(\epsilon_1+1)^2 + \epsilon_2^2]$  is shown also.

The effective number of electrons per atom contributing to absorption processes below energy  $E$  can be calculated from the oscillator-strength sum rule, given by

$$N_{\text{eff}}(E) = \frac{2}{\pi} \frac{1}{(\hbar\omega_p)^2} \int_0^E \epsilon_2(E') E' dE',$$

where  $\hbar\omega_p$  is the free-electron plasma energy, 19.56 eV, as calculated from  $(\omega_p)^2 = 4\pi Ne^2/m$ , there being  $N$  electrons of mass  $m$  per unit volume.  $N_{\text{eff}}$  rises from zero with plateaus at about 1.5, 10, and 26 eV.  $N_{\text{eff}}$  appears to level off at 26 eV, with a value of about 6.2 electrons per atom. Above about 26 eV, effects from core transitions become important.

### III. DISCUSSION

Band calculations were performed for Nb by Mattheiss<sup>7</sup>: a nonrelativistic augmented-plane-wave (APW) approach was taken and the muffin-tin potentials were derived from superposed atomic charge densities. Ta was also considered and the two group-VB transition metals were compared. A comparison with the bands of Deegan and Twose,<sup>6</sup> who used a modified orthogonalized-plane-wave (OPW) method, shows that the over-all agreement is excellent. Agreement with experiment has also

been good, as shown by the de Haas-van Alphen measurements on Nb and Ta by Halloran *et al.*<sup>14</sup> In Fig. 5 we reproduce the energy-band results of Mattheiss.

In Fig. 1 the absorptivity spectrum was displayed for the low-energy region. It was concluded above that interband effects are structureless below the 1.0-eV onset. The band scheme shows that indeed the only transitions along symmetry lines which could be identified as those seen by GLMS are  $\Sigma_2 \rightarrow \Sigma_1$  transitions. For a bcc crystal, the electric dipole selection rules forbid such transitions, but spin-orbit effects cause these to become allowed  $\Sigma_5 \rightarrow \Sigma_5$  transitions. Because spin-orbit effects are not large in Nb, these transitions should be weak.

In Fig. 3, structure is observed in  $\epsilon_2$  at about 2.4 eV. While the transitions  $\Sigma_2 \rightarrow \Sigma_1$  are forbidden,  $\Sigma_1 \rightarrow \Sigma_1$  are allowed and a tentative identification can be made for the 2.4-eV structure as originating from the upper  $\Sigma_1 \rightarrow \Sigma_1$  lines and nearby regions of  $\vec{k}$  space. Such a transition is strong, as evidenced by the large density of states of the two bands involved, particularly where  $\Sigma_1$  dips below the Fermi level. Likewise, weaker transitions can be expected from  $\Gamma_1 \rightarrow \Gamma'_{25}$  at 5.7 eV,  $D_4 \rightarrow D_1$  at 4.2 eV, and  $\Delta_1 \rightarrow \Delta'_2$  at about 4.4 eV, which might account for the experimental structure that occurs at about those energies. Also entering weakly could be transitions along the directions  $\Gamma_1 - \Lambda_1 \rightarrow \Gamma'_{25} - \Lambda_1$ , which must be weak because the bands are only roughly parallel. Above 6 eV it becomes increasingly difficult to make even tentative as-

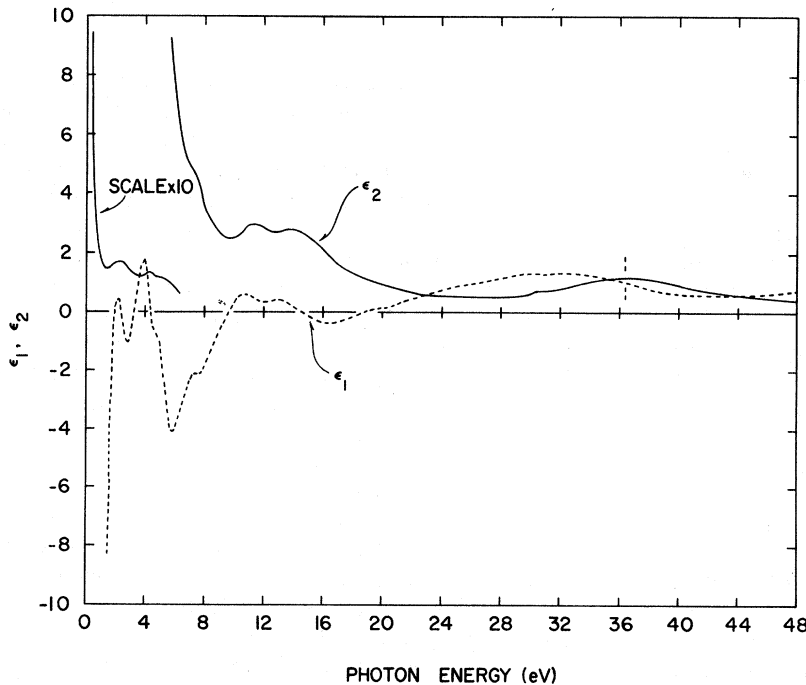


FIG. 3. Dielectric constants of niobium. The vertical dashed line at 36.4 eV corresponds to the limit of our reflectivity data. Above about 21 eV, the constants become less reliable due to the high-energy extrapolation.

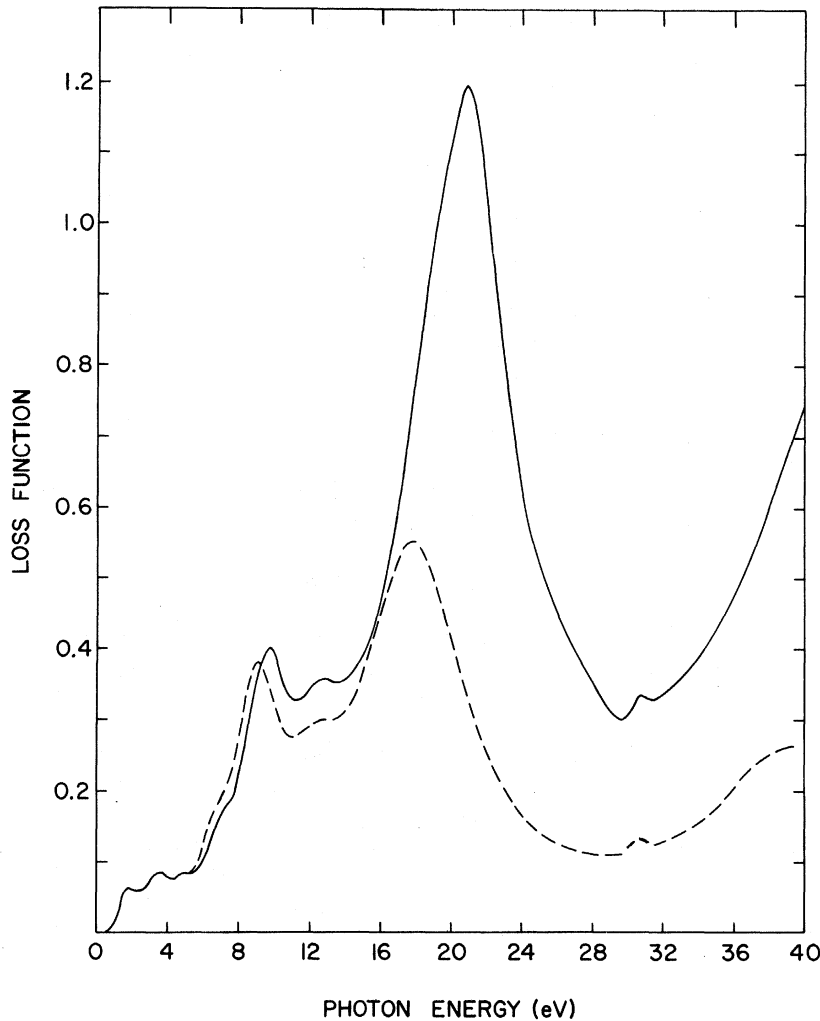


FIG. 4. Electron energy-loss function for niobium. Solid line, bulk,  $\text{Im}(-1/\bar{\epsilon})$ ; dashed line, surface,  $\text{Im}[-1/(\bar{\epsilon} + 1)]$ . The reflectivity extrapolation was adjusted to produce the peak in the loss function at 43.2 eV.

signments of the structures of Fig. 3. In particular, it would be difficult to discuss the origin of the structure between 10 and 15 eV. This structure could arise from transitions from the large density of filled states below the Fermi energy to a region of fairly high density of states about 10 eV above the Fermi energy or from delayed  $4d \rightarrow f$  transitions. The latter effect, often observed for  $d$ -like core levels in both atoms and solids,<sup>22</sup> arises from the effect of the centrifugal potential on the dipole matrix elements via the radial part of the wave functions.<sup>24</sup> Similar structure in  $\epsilon_2$  occurs in Cr.<sup>25</sup>

Nb has  $N_{II-III}$  core levels about 34 eV below the Fermi energy.<sup>26</sup> The onset of transitions from these levels probably accounts for the rise in reflectivity above 28 eV. Because of the inaccuracies in the extrapolation, no quantitative information can be gained about these transitions from our data.

In Fig. 4 the volume loss function displays struc-

ture below about 8 eV, which corresponds to structure in  $\epsilon_2$  and can be identified as arising from interband effects. However, the peak at 9.7 eV corresponds to a minimum in  $\epsilon_2$  and a crossing of the axis by  $\epsilon_1$ , with  $d\epsilon_1/dE > 0$ . This can be identified as a plasmon structure. The existence of this structure has already been noted by Apholte and Ulmer,<sup>27</sup> who measured characteristic energy losses in Nb. They reported structure at  $9.9 \pm 1.0$  eV. However, they did not measure the loss function itself, so separation into interband and collective effects is difficult from their data alone. The surface loss function shows a maximum of comparable strength at 9.0 eV, corresponding to surface-plasmon excitation.

In the structure of  $\epsilon_2$ , one observes a slight shoulder at about 20 eV;  $\epsilon_1$  is seen to be small at this point, having crossed the axis at about 18.9 eV, and displays a kink near 20.8 eV. This behavior manifests itself in the volume loss function by a strong resonance at 20.8 eV. The surface

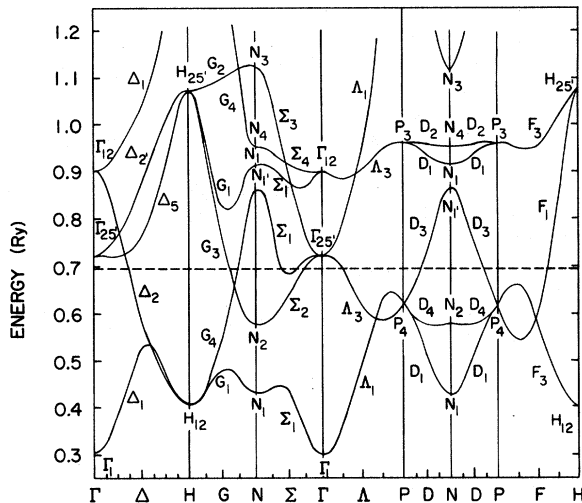


FIG. 5. Energy-band structure of niobium from Ref. 7.

loss function exhibits a weaker peak at 17.7 eV. These can be compared with the results of Apholte and Ulmer,<sup>27</sup> who observed a peak at  $19.7 \pm 1.4$  eV. Their peak should be a composite of surface and volume loss function peaks. Because the magnitudes of our  $\tilde{\epsilon}$  may not be correct above 21 eV, the position of this peak in our data is not known very well and the uncertainty is difficult to estimate. For a free-electron gas with the parameters of Nb, the plasma energy is calculated to be 19.56 eV; it is apparent that the resonance frequency has been shifted to higher energy due to interband absorption at lower energy.

Energy-loss measurements have also been performed by Lynch and Swan.<sup>28</sup> They report peaks in the loss function at 9.5 and 19.6 eV, in agreement with Ref. 27. Structure was also found at 32.4 eV and was identified as due to the  $N_{II-III}$  core transitions; this agrees well with our optical results (see Fig. 4).

In addition to the peaks at 9.9 and 19.7 eV, Apholte and Ulmer identified a resonance at  $43.3 \pm 0.2$  eV. Use was made of this information when

a high-energy extrapolation was made in our KK analysis of the reflectivity data. As seen from Fig. 2, the reflectivity is rising at the upper limit of our data. Since the position of the peak in  $R$  was not known, a variety of different extrapolations were introduced. The one which was chosen produced a peak in the loss function at 43.2 eV. This is shown in Fig. 2. An extrapolation which gave  $R$  a  $7\frac{1}{2}\%$  peak at 42 eV produced a loss function peak at 46 eV. The magnitude of  $\epsilon_1$  was changed by less than 1% below 35 eV;  $\epsilon_2$  was changed by less than 2% below 28 eV, but the uncertainty was as high as 8% at 35 eV. The uncertainties due to the high-energy extrapolation are propagated in the calculation of  $R$  at  $45^\circ$  and  $60^\circ$ , and are probably the source of disagreement between experimental and calculated reflectivity values at these angles.

#### CONCLUSION

The reflectivity spectrum presented here covers a broad energy range and represents a considerable improvement over existing data; not only is it continuous, but it extends the ultraviolet range from about 14.3 to 36.4 eV. Optical constants have been calculated using a KK integral technique and the resulting structure in the dielectric function has been identified tentatively in conjunction with the results of Mattheiss.

#### ACKNOWLEDGMENTS

The authors thank F. A. Schmidt for providing the Nb ingot, G. V. Austin, E. L. DeKalb, and N. M. Neymer for performing the chemical analyses, and H. H. Baker for his assistance in preparing the crystals for study. Discussions with L. Hodges and D. K. Finnemore are gratefully acknowledged. The accuracy of some of the measurements was enhanced by the gold-mirror calibration kindly performed by J. M. Bennett. The cooperation of the storage-ring staff, especially E. M. Rowe, C. H. Pruet, and R. Otte, is appreciated. The storage ring is supported by the U. S. Air Force Office of Scientific Research.

<sup>1</sup>T. L. Loucks, *Augmented Plane Wave Method* (Benjamin, New York, 1967).

<sup>2</sup>W. A. Harrison, *Pseudopotentials in The Theory of Metals* (Benjamin, New York, 1966).

<sup>3</sup>V. Heine, M. L. Cohen, and D. Weaire, in *Solid State Physics* (Academic, New York, 1970), Vol. 24.

<sup>4</sup>J. M. Ziman, in *Solid State Physics* (Academic, New York, 1970), Vol. 24.

<sup>5</sup>L. Hodges, R. E. Watson, and H. Ehrenreich, *Phys. Rev. B* **5**, 3953 (1972).

<sup>6</sup>R. A. Deegan and W. D. Twose, *Phys. Rev.* **164**, 993 (1967).

<sup>7</sup>L. F. Mattheiss, *Phys. Rev. B* **1**, 373 (1970).

<sup>8</sup>M. M. Kirillova, *Zh. Eksp. Teor. Fiz.* **61**, 336 (1971) [*Sov. Phys. JETP* **34**, 178 (1972)].

<sup>9</sup>M. Ph. Stoll (private communication).

<sup>10</sup>A. I. Golovashkin, I. E. Leksina, G. P. Motulevich, and A. A. Shubin, *Zh. Eksp. Teor. Fiz.* **56**, 51 (1969) [*Sov. Phys. JETP* **29**, 27 (1969)].

<sup>11</sup>F. I. Vilesov, A. A. Azgrubskii, and M. M. Kirillova, *Optika i Spektros.* **23**, 153 (1967) [*Opt. Spectrosc.* **23**, 79 (1967)].

<sup>12</sup>M. M. Kirillova and B. A. Charikov, *Fiz. Metal. Metalloved.* **19**, 495 (1965).

<sup>13</sup>E. Fawcett, W. A. Reed, and R. R. Soden, *Phys. Rev.* **159**, 533 (1967).

<sup>14</sup>M. H. Halloran, J. H. Condon, J. E. Graebner, J. E. Kunzler, and F. S. L. Hsu, *Phys. Rev. B* **1**, 366 (1970).

<sup>15</sup>A. C. Thorson and T. G. Berlincourt, *Phys. Rev. Letters* **7**, 244 (1961); G. B. Scott, M. Springfield, and

J. R. Stockton, Phys. Letters 27, 655 (1961).

<sup>16</sup>P. L. Hartman and E. Logothetis, Appl. Opt. 3, 255 (1964).

<sup>17</sup>The reflectometer was calibrated using a gold mirror whose reflectivity was previously measured with an accuracy exceeding 0.1%. This reduced our uncertainty from about 10% to the 2% quoted above.

<sup>18</sup>L. W. Bos and D. W. Lynch, Phys. Rev. B 2, 4784 (1970).

<sup>19</sup>J. H. Weaver, D. W. Lynch, and R. Rosei, Phys. Rev. B 5, 2829 (1972).

<sup>20</sup>R. J. Bartlett, D. W. Lynch, and R. Rosei, Phys. Rev. B 3, 4074 (1971).

<sup>21</sup>L. W. Bos and D. W. Lynch, Phys. Rev. Letters 25, 156 (1970).

<sup>22</sup>D. W. Lynch, R. Rosei, and J. H. Weaver, Solid State Commun. 9, 2195 (1971).

<sup>23</sup>J. L. Dehmer, A. F. Starace, U. Fano, J. Sugar, and J. W. Cooper, Phys. Rev. Letters 26, 1521 (1971), and references therein.

<sup>24</sup>U. Fano and J. W. Cooper, Rev. Mod. Phys. 40, 441 (1968).

<sup>25</sup>D. W. Lynch and C. G. Olson (unpublished).

<sup>26</sup>J. A. Bearden and A. F. Burr, Rev. Mod. Phys. 39, 125 (1967).

<sup>27</sup>H. R. Apherholte and K. Ulmer, Phys. Letters 22, 552 (1966).

<sup>28</sup>M. J. Lynch and J. B. Swan, Aust. J. Phys. 21, 811 (1968).

## Classical Linear-Chain Hubbard Model: Metal-Insulator Transition\*

Robert A. Bari

Brookhaven National Laboratory, Upton, New York 11973

(Received 7 December 1972)

The linear-chain Hubbard model with nearest-neighbor hopping parameter  $t$  is reexpressed in terms of pseudospin operators according to the Jordan-Wigner transformation. The resulting spin model is then treated classically. It is found that for a half-filled band there is a phase transition in the ground state as a function of  $t$ . The electrical conductivity is calculated and shown to vanish discontinuously at the critical value of  $4t = U$  (Coulomb repulsion). A Josephson-type relation is obtained between the difference in azimuthal angles of adjacent spins and the potential difference between sites. It is also shown that a local magnetic moment exists in the insulating state. For the non-half-filled band, it is shown that the ground state is ferromagnetic for  $4t < U$ .

The one-dimensional Hubbard model<sup>1</sup> is written as

$$H = -t \sum_{i,\sigma} (C_{i\sigma}^\dagger C_{i+1\sigma} + \text{H. c.}) + U \sum_i n_{i\uparrow} n_{i\downarrow}. \quad (1)$$

The hopping  $t$  is among nearest neighbors.  $C_{i\sigma}^\dagger$  creates an electron on site  $R_i$  with spin  $\sigma$ ;  $n_{i\sigma} = C_{i\sigma}^\dagger C_{i\sigma}$ .  $U$  is the intrasite Coulomb repulsion.

The Jordan-Wigner transformation<sup>2</sup> is applied to  $H$ . We define (with  $N$  = number of sites)

$$S_i^x = C_{i\uparrow}^\dagger \exp \left[ i\pi \left( \sum_{j=1}^N n_{j\uparrow} + \sum_{j=1}^{i-1} n_{j\downarrow} \right) \right], \quad (2)$$

$$T_i^x = C_{i\uparrow}^\dagger \exp \left[ i\pi \sum_{j=1}^{i-1} n_{j\downarrow} \right]. \quad (3)$$

Here  $S_i^x = S_i^x + iS_i^y$ ,  $T_i^x = T_i^x + iT_i^y$ , and it also follows that  $S_i^z = n_{i\uparrow} - \frac{1}{2}$  and  $T_i^z = n_{i\downarrow} - \frac{1}{2}$ . The vector operators  $\vec{S} = (S^x, S^y, S^z)$  and  $\vec{T} = (T^x, T^y, T^z)$  are each spin- $\frac{1}{2}$  operators and satisfy the usual angular momentum commutator algebra. In terms of the spin operators  $H$  is written as<sup>3</sup>

$$H = -2t \sum_i (S_i^x S_{i+1}^x + S_i^y S_{i+1}^y + T_i^x T_{i+1}^x + T_i^y T_{i+1}^y) + U \sum_i S_i^z T_i^z + \frac{1}{2} U \sum_i (S_i^z + T_i^z) + \frac{1}{4} NU. \quad (4)$$

The Hubbard model is now in the form of the sum of two spin- $\frac{1}{2}$  XY models; each is in a transverse uniform magnetic field and the  $z$  components of the two spin systems are coupled by an intrasite exchange. The equivalence of (a class of models of) an interacting, one-dimensional electron gas to a spin model was discussed by Lieb and Mattis.<sup>4</sup>

Although the equivalence allows one to regard the Hubbard model from a different point of view, the transformation to the spin variables does not lead to an apparent simplification of the problem (but its usefulness is illustrated in Ref. 4). In this paper, we use the spin equivalence to generalize the Hubbard model to arbitrary spin. In particular, we study the classical-spin limit of Eq. (4). The connection with the original spin- $\frac{1}{2}$  problem is now remote and in fact we expect the two systems to have qualitative differences. The classical Hubbard model can be thought of as a system of interacting multidegenerate bands in the limit of an infinite number of bands. The band model thus obtained [by working back to a set of fermion operators from the classical-spin generalization of Eq. (4)] is not completely realistic since it does not sort out Hund's-rule effects, allows intersite, interband hopping of electrons and includes interac-